



Article

# Hepatoprotective Effect of Aqueous Extract from the Seeds of *Orychophragmus violaceus* against Liver Injury in Mice and HepG2 Cells

Xiaowei Huo <sup>1,†</sup>, Chenqi Liu <sup>1,2,†</sup>, Li Gao <sup>1</sup>, Xudong Xu <sup>1</sup>, Nailiang Zhu <sup>1,\*</sup> and Li Cao <sup>1,\*</sup>

<sup>1</sup> Institute of Medicinal Plant Development, Chinese Academy of Medical Sciences and Peking Union Medical College, Beijing 100193, China; huoxiaoweiforever@163.com (X.H.); chenqiliu1@163.com (C.L.); gli1986@163.com (L.G.); xdxu@implad.ac.cn (X.X.)

<sup>2</sup> Research Center on Life Sciences and Environmental Sciences, Harbin University of Commerce, Harbin 150076, China

\* Correspondence: zhu13liang@126.com (N.Z.); lcao@implad.ac.cn (L.C.); Tel.: +86-10-5783-3222 (N.Z. & L.C.)

† These authors contributed equally to this work.

Academic Editor: David Arráez-Román

Received: 11 April 2017; Accepted: 24 May 2017; Published: 15 June 2017

**Abstract:** *Orychophragmus violaceus* (*O. violaceus*) is a kind of edible wild herb in north China and its seeds have medical potential, however, the effect of *O. violaceus* seeds on liver injury and the mechanism of action remains poorly understood. Thus, the purpose of the present study is to investigate the effect of *O. violaceus* seeds on liver injury and further explore the molecular mechanism of the beneficial effects using aqueous extract from the seeds of *O. violaceus* (AEOV). Mice were orally administrated with saline, AEOV, and biphenyldicarboxylate for 4 days, and were then injected subcutaneously with 0.1% carbon tetrachloride (CCl<sub>4</sub>) dissolved in corn oil. Sixteen hours later, mice were sacrificed and blood samples were collected. Then, the serum was separated and used for biochemical assay. Livers were excised and were routinely processed for histological examinations. Enzyme activities and protein levels in liver homogenates were detected using commercial kits or by western blot analysis. Additionally, the hepatoprotective effect of AEOV in vitro was evaluated using epigoitrin, the major alkaloid compound isolated from AEOV. We found that AEOV attenuated liver injury induced by CCl<sub>4</sub> as evidenced by decreased levels of alanine aminotransferase (ALT) and aminotransferase (AST) in serum, improvement of liver histopathological changes, and substantial attenuation of oxidative stress and inflammation via regulation of nuclear factor-erythroid 2-related factor-2 (Nrf2) and nuclear factor κB (NFκB) pathways. These effects of AEOV were comparable to that of biphenyldicarboxylate which was commonly used as a hepatoprotective reference. Moreover, pretreatment of HepG2 cells with epigoitrin improved cell viability, decreased lactate dehydrogenase (LDH) and malondialdehyde (MDA) levels, increased superoxide dismutase (SOD) and glutathione peroxidase (GSH-Px) activity, attenuated the NFκB pathway, and elevated the Nrf2 pathway after exposure to H<sub>2</sub>O<sub>2</sub>. These results suggest that AEOV could effectively prevent CCl<sub>4</sub>-induced liver injury in mice via regulating the Nrf2 and NFκB pathways, and reveal the cytoprotective effects of epigoitrin against H<sub>2</sub>O<sub>2</sub>-induced oxidative stress in HepG2 cells.

**Keywords:** *Orychophragmus violaceus*; epigoitrin; hepatoprotective effect; anti-inflammation; antioxidant

## 1. Introduction

Liver injury, generally caused by viral hepatitis, non-alcoholic steatohepatitis, alcohol abuse, and drug intoxication [1,2], has severe consequences for metabolism, detoxification, immune response, and antimicrobial defense because the liver is involved in almost all vital biological processes. The

mechanism of liver injury is not well established, however, emerging evidence suggests that multiple mechanisms are postulated to be involved in the development of liver injury such as oxidative stress, dysfunction of intracellular targets, and inflammation, as well as complex interactions between alcohol metabolism, multiple cytokines, and the innate immune system [3–5]. Oxidative stress and inflammatory action, based on the involvement of the transcription factor nuclear factor-erythroid 2-related factor-2 (Nrf2) and transcription factor nuclear factor  $\kappa$  B (NF $\kappa$ B), have gained increasing attention largely due to their critical roles in the initiation and progression of liver injury [6–8]. Recent studies have suggested that the activation of nuclear factor-erythroid 2-related factor-2–antioxidant response element (Nrf2–ARE) signaling can confer protection to normal cells or tissues by preventing free radical stress [9–11]. Additionally, suppression of the NF $\kappa$ B pathway has been found to be essential for the controlling of the expression of pro-inflammatory cytokines which, otherwise, may contribute to tissue damage [12,13]. In this regard, we hypothesize that approaches and drugs successfully used in controlling oxidative stress and inflammation may help protect against liver injury.

In recent years, a number of drugs with anti-oxidative and anti-inflammatory properties have been evaluated as hepatoprotective agents, however, they generally have been proven to be nonspecific and exhibited limited efficacy in the therapy of liver injury [14,15]. Herein, it is necessary to explore more potential agents for the treatment of liver injury, and natural products derived from traditional Chinese herbal medicines may provide alternative treatment options for liver injury. Actually, numerous studies have emphasized the use of natural products for the prevention and therapy of liver injury because of their safety and efficacy as an alternative remedy compared with chemically synthesized drugs [16]. *Orychophragmus violaceus*, also called Eryuelan in China, is a kind of edible wild herb in north China which is rich in linoleic acid favorable for the body. This species has been reported to be valuable due to its high seed yield potential and good quality of seed oil [17]. The seeds of *O. violaceus* also have potential for the treatment of liver disease [18], however, the effect of *O. violaceus* seeds for liver injury induced by CCl<sub>4</sub> is not clear, and the underlying mechanism of the potential effect remains to be elucidated.

The current study was, therefore, designed to evaluate the hepatoprotective effect of aqueous extract from the seeds of *O. violaceus* (AEOV) both in vivo and in vitro. In this study, the mouse model of CCl<sub>4</sub>-induced hepatic injury was established to investigate the hepatoprotective effect of AEOV in vivo and elucidate the underlying mechanisms. Furthermore, the hepatoprotective effect of epigoitrin in vitro was evaluated using epigoitrin in H<sub>2</sub>O<sub>2</sub>-induced HepG2 cells. The results showed that the acute liver injury induced by CCl<sub>4</sub> treatment was significantly attenuated by AEOV treatment compared with untreated mice as determined by the reduced serum levels of aspartate aminotransferase (AST) and alanine aminotransferase (ALT), and less severe liver injury. Epigoitrin, the major alkaloid compound isolated from AEOV, exhibited a strong cytoprotective effect against H<sub>2</sub>O<sub>2</sub>-induced oxidative damage in HepG2 cells. With regard to the possible mechanism, our data revealed that AEOV ameliorated liver injury by decreasing oxidative damage and inhibiting the production of pro-inflammatory cytokine tumor necrosis factor (TNF)- $\alpha$  via regulation of Nrf2 and NF $\kappa$ B signaling pathways. The cytoprotective effect of epigoitrin was also associated with Nrf2 and NF $\kappa$ B pathways. These results highlight the potential of AEOV in the treatment of liver injury.

## 2. Results

### 2.1. High Performance Liquid Chromatography (HPLC) Analysis and Composition of AEOV

The chromatographic profiles of the components of the AEOV were analyzed using high performance liquid chromatography (HPLC) as shown in Figure 1A. Data in Figure 1B show the chemical structure of some exact composition of the mixture. Compounds 1–14 were identified to be epigoitrin (1); *N*-2-hydroxy-3-butenyl-benzamide (2); 2-Amino-5-hydroxybenzoic acid (3); *N*-benzoyl-epigoitrin (4);  $\alpha$ -(2-carboxyacetyl) amino]-benzeneacetic acid (5); 3-phenyl-6-

vinylmorpholin-2-one (6); adenosine (7); 2'-deoxy adenosine (8); blumenol A (9); protocatechuic acid (10); salicylic acid (11); caffeic acid (12); (+)-catechin (13); and *p*-coumaric acid (14).

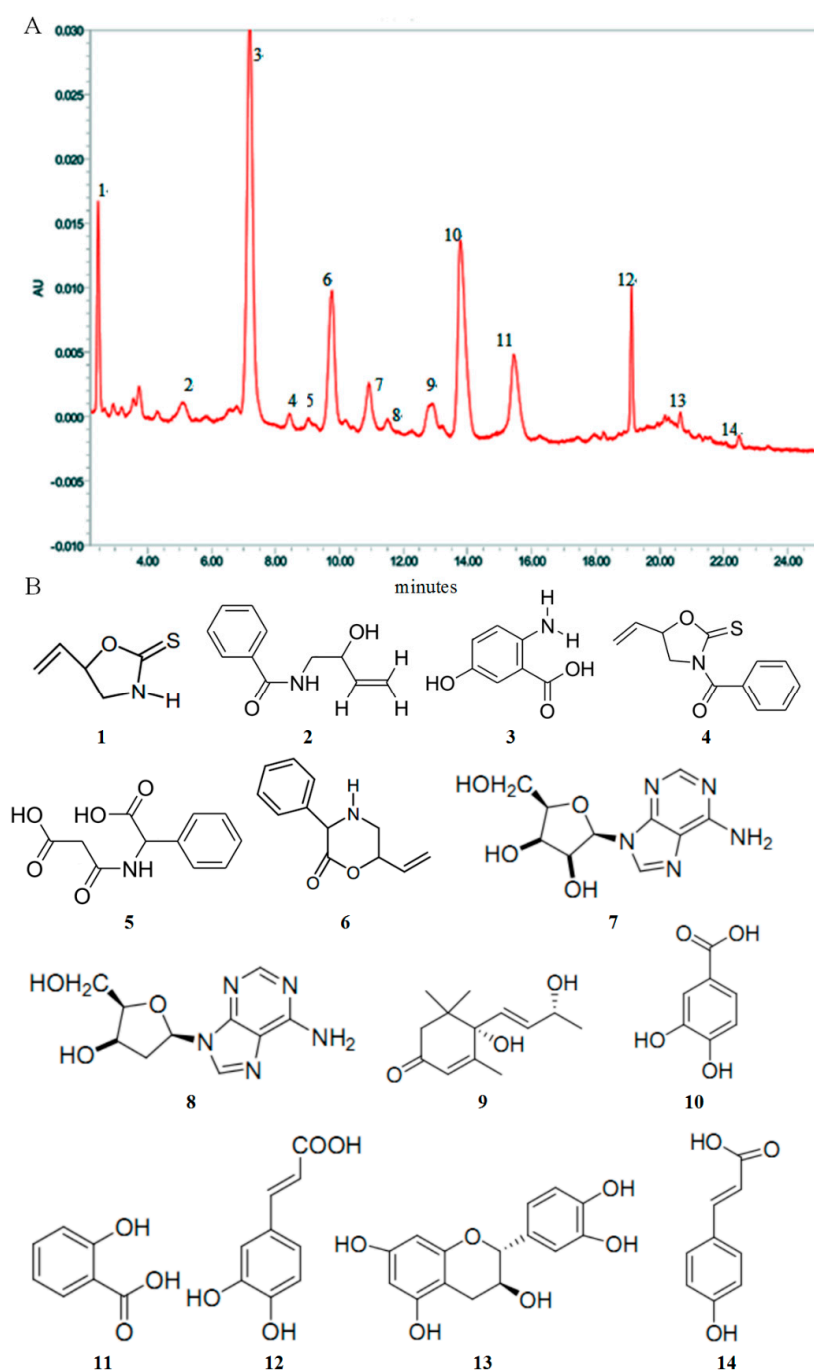


**Figure 1.** (A) The chromatographic profile of aqueous extract from *Orychophragmus violaceus* (AEOV) analyzed by HPLC; (B) Chemical structure of the main constituents of AEOV.

## 2.2. Hepatoprotective Effect of AEOV against $\text{CCl}_4$ -Induced Liver Injury

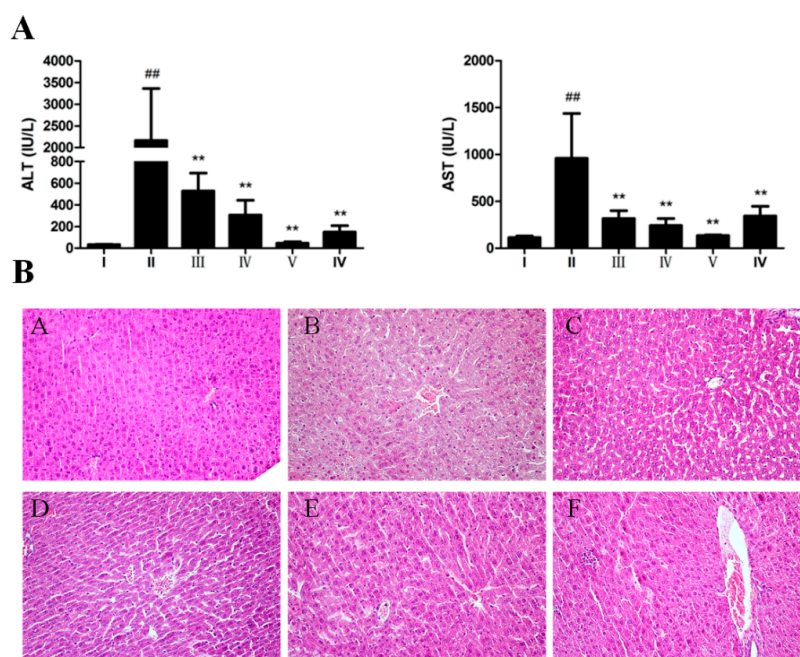
We established animal model of hepatic injury by intraperitoneal injection of  $\text{CCl}_4$  in Balb/c mice. As shown in Table 1,  $\text{CCl}_4$  injection and AEOV administration had no significant effect on body weight and liver index. Biochemical indicators including AST and ALT were detected in all treatment groups to evaluate the hepatoprotective effect of AEOV. As shown in Figure 2A, serum levels of AST and ALT, which were commonly used as biomarkers for liver injury, were significantly elevated in mice injected

with  $\text{CCl}_4$  compared to the control group. Fortunately, AEOV treatment dramatically reduced both of these two indicators. The hepatoprotective effect of AEOV was also assessed by morphological observation of hematoxylin and eosin (H&E)-stained liver tissues. As shown in Figure 2B, histological examination results were well consistent with that of the biochemical parameters. Multifocal hepatic parenchymal necrosis with inflammatory cell infiltration was observed in  $\text{CCl}_4$ -induced mice. AEOV and biphenyldicarboxylate treatment significantly ameliorated the degree of hepatic parenchymal necrosis and inflammatory cell infiltration was also attenuated.

**Table 1.** Effect of AEOV on body weight and liver index in mice.

Group	Dose (mg/kg)	Body Weight (g)	Relative Liver Weight (g/100 g Body Weight)
I	-	19.7 ± 0.89	4.67 ± 0.17
II	-	20.13 ± 0.6	5.02 ± 0.22
III	125	19.21 ± 0.91	4.65 ± 0.39
IV	250	19.68 ± 0.65	4.85 ± 0.16
V	500	19.85 ± 0.76	4.84 ± 0.22
VI	150	20.6 ± 0.8	5.13 ± 0.21

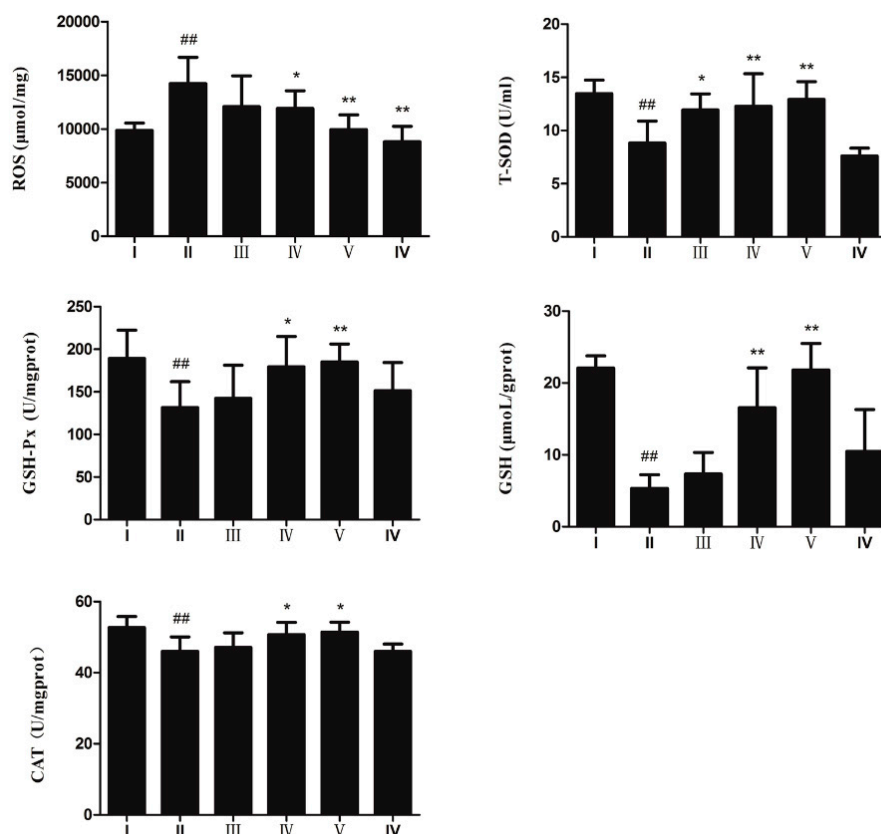
I: saline; II: saline +  $\text{CCl}_4$ ; III: AEOV 125 mg/kg +  $\text{CCl}_4$ ; IV: AEOV 250 mg/kg +  $\text{CCl}_4$ ; V: AEOV 500 mg/kg +  $\text{CCl}_4$ ; VI: biphenyldicarboxylate 150 mg/kg +  $\text{CCl}_4$ .



**Figure 2.** The effect of AEOV on  $\text{CCl}_4$ -induced liver injury. (A) Serum levels of alanine aminotransferase (ALT) and aminotransferase (AST). Groups are as follows. I: saline; II: saline +  $\text{CCl}_4$ ; III: AEOV 125 mg/kg +  $\text{CCl}_4$ ; IV: AEOV 250 mg/kg +  $\text{CCl}_4$ ; V: AEOV 500 mg/kg +  $\text{CCl}_4$ ; VI: biphenyldicarboxylate 150 mg/kg +  $\text{CCl}_4$ . Values are the means ± standard error of the mean (SEM) of three independent experiments. ##  $p < 0.01$  versus normal control group, \*\*  $p < 0.01$  versus  $\text{CCl}_4$ -treated group; (B) Hematoxylin and eosin (H&E) staining of livers. Mice were treated with saline, AEOV (125, 250, and 500 mg/kg), and biphenyldicarboxylate 150 mg/kg for 4 days, and were then injected subcutaneously with 0.1%  $\text{CCl}_4$  dissolved in corn oil. Sixteen hours later, mice were sacrificed and livers were excised and stained with hematoxylin and eosin (400×). Groups are as follows. A: saline; B: saline +  $\text{CCl}_4$ ; C: AEOV 125 mg/kg +  $\text{CCl}_4$ ; D: AEOV 250 mg/kg +  $\text{CCl}_4$ ; E: AEOV 500 mg/kg +  $\text{CCl}_4$ ; F: biphenyldicarboxylate 150 mg/kg +  $\text{CCl}_4$ .

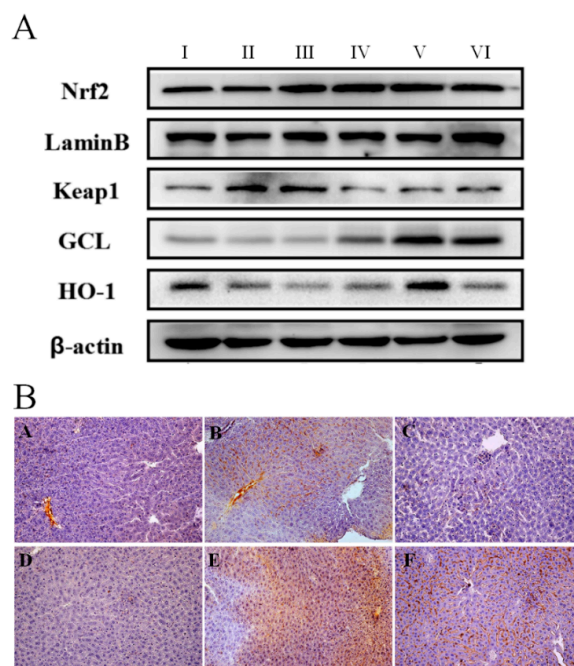
### 2.3. Anti-Oxidative Effect of AEOV on Liver Tissues

Figure 3 shows that  $\text{CCl}_4$  administration markedly increased the hepatic reactive oxygen species (ROS) level. The AEOV pre-treatment group significantly ameliorated the production of ROS in liver tissues. Anti-oxidative enzyme activity was also tested to evaluate the anti-oxidative effect of AEOV. Superoxide dismutase (T-SOD), catalase (CAT), glutathione peroxidase (GSH-Px), and glutathione (GSH) levels in liver homogenates were significantly decreased in the  $\text{CCl}_4$ -treated mice (group II) relative to that of the control group (group I). However, the administration of AEOV significantly reversed  $\text{CCl}_4$ -induced decrease of T-SOD, CAT, GSH-Px, and GSH, thus partially suggesting its anti-oxidative effect on the  $\text{CCl}_4$ -induced model.



**Figure 3.** Levels of reactive oxygen species (ROS), superoxide dismutase (T-SOD), glutathione (GSH), glutathione peroxidase (GSH-Px), and catalase (CAT) in liver tissues. Groups are as follows. I: saline; II: saline +  $\text{CCl}_4$ ; III: AEOV 125 mg/kg +  $\text{CCl}_4$ ; IV: AEOV 250 mg/kg +  $\text{CCl}_4$ ; V: AEOV 500 mg/kg +  $\text{CCl}_4$ ; VI: biphenyldicarboxylate 150 mg/kg +  $\text{CCl}_4$ . Values are the means  $\pm$  SEM of three independent experiments. <sup>##</sup>  $p < 0.01$  versus normal control group, <sup>\*\*</sup>  $p < 0.01$ , <sup>\*</sup>  $p < 0.05$  versus  $\text{CCl}_4$ -treated group.

We next sought to determine possible mechanisms for the onset of antioxidant by examining the effect of AEOV on Nrf2 signaling. Results presented in Figure 4A show that AEOV administration significantly down-regulated expression of Kelch-like ECH-associated protein 1 (Keap1), an inhibitor of Nrf2, substantially enhanced accumulation of Nrf2 in nuclei, and markedly increased expression of glutamate cysteine ligase (GCL) and heme oxygenase (HO)-1. Moreover, immunohistochemical examination confirmed the increased expression of Nrf2 in liver tissues after AEOV administration (Figure 4B), which was consistent with the results of western blot. These data strongly demonstrated the anti-oxidative property of AEOV *in vivo* via the activation of Nrf2 pathway by activating Nrf2/inactivating Keap1 accompanied with the elevation of anti-oxidative enzyme activity.



**Figure 4.** Anti-oxidative effect of AEOV on liver tissues. (A) Liver tissues were collected and used to analyze the expression of nuclear factor-erythroid 2-related factor-2 (Nrf2), Kelch-like ECH-associated protein 1 (Keap1), heme oxygenase (HO), and glutamate cysteine ligase (GCL) by western blot analysis. Groups are as follows. I: Saline; II: saline + CCl<sub>4</sub>; III: AEOV 125 mg/kg + CCl<sub>4</sub>; IV: AEOV 250 mg/kg + CCl<sub>4</sub>; V: AEOV 500 mg/kg + CCl<sub>4</sub>; VI: biphenyldicarboxylate 150 mg/kg + CCl<sub>4</sub>; (B) Immunohistochemical staining of Nrf2 in liver tissues (400×). Groups are as follows. A: saline; B: saline + CCl<sub>4</sub>; C: AEOV 125 mg/kg + CCl<sub>4</sub>; D: AEOV 250 mg/kg + CCl<sub>4</sub>; E: AEOV 500 mg/kg + CCl<sub>4</sub>; F: biphenyldicarboxylate 150 mg/kg + CCl<sub>4</sub>.

#### 2.4. Anti-Inflammatory Effect of AEOV on Liver Tissues

It is well known that modulation of the pro-inflammatory response plays a critical role in liver injury. Consistently, our results in Figure 5A showed that the level of pro-inflammatory cytokine TNF- $\alpha$  was significantly increased after CCl<sub>4</sub> injection. AEOV significantly attenuated CCl<sub>4</sub>-induced increase of TNF- $\alpha$ , thereby indicating that AEOV exerted potent anti-inflammatory effect. Biphenyldicarboxylate produced mild decrease in the level of TNF- $\alpha$ .

AEOV exhibited anti-inflammatory activity by the inhibition of NF $\kappa$ B pathway. As shown in Figure 5B, CCl<sub>4</sub> injection significantly increased expression of I $\kappa$ B kinase  $\alpha$  (IKK $\alpha$ ) and phosphorylated inhibitory factor kappaB-alpha (p-I $\kappa$ B $\alpha$ ), and promoted nuclear translocation of NF $\kappa$ B in liver tissues when compared to normal mice. Treatment with AEOV or biphenyldicarboxylate significantly reduced expression of IKK $\alpha$  and p-I $\kappa$ B $\alpha$ , and attenuated NF $\kappa$ B translocation to nuclei compared to CCl<sub>4</sub>-induced mice without AEOV treatment. Additionally, we performed an immunohistochemical examination using an antibody against NF $\kappa$ B. Data shown in Figure 5C were well consistent with western blotting analysis, demonstrating that AEOV attenuated CCl<sub>4</sub>-induced NF $\kappa$ B translocation, which may have contributed to the decreased secretion of proinflammatory cytokine TNF- $\alpha$ .

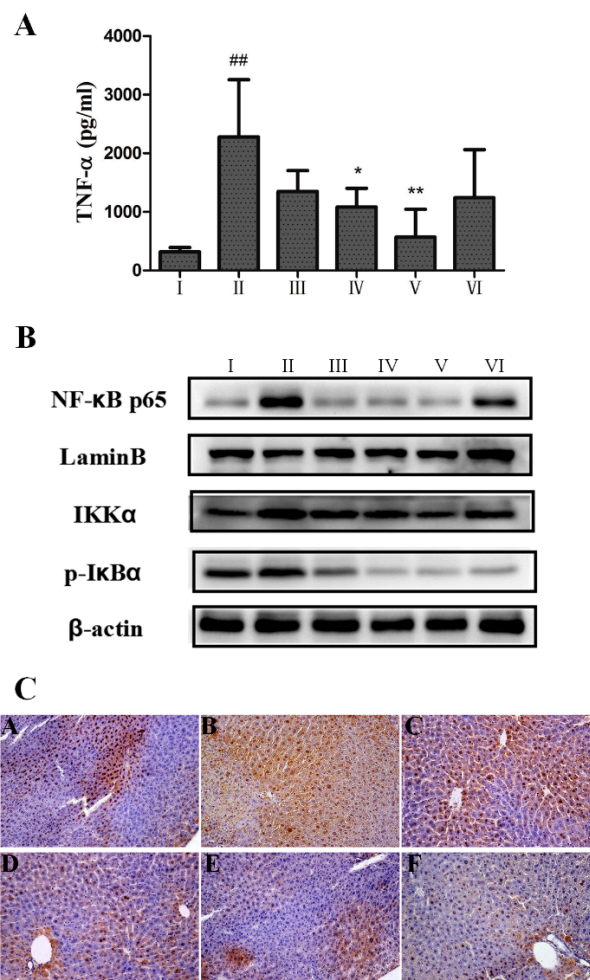


**Figure 5.** Anti-inflammatory effect of AEOV on liver tissues. (A) Serum tumor necrosis factor (TNF) $\alpha$  level. Groups are as follows. I: saline; II: saline + CCl<sub>4</sub>; III: AEOV 125 mg/kg + CCl<sub>4</sub>; IV: AEOV 250 mg/kg + CCl<sub>4</sub>; V: AEOV 500 mg/kg + CCl<sub>4</sub>; VI: biphenyldicarboxylate 150 mg/kg + CCl<sub>4</sub>. Values are the means  $\pm$  SEM of three independent experiments.  $## p < 0.01$  versus normal control group,  $** p < 0.01$ ,  $* p < 0.05$  versus CCl<sub>4</sub>-treated group; (B) Western blot analysis of nuclear factor  $\kappa$  B (NF $\kappa$ B), I $\kappa$ B kinase  $\alpha$  (IKK $\alpha$ ), and phosphorylated inhibitory factor kappaB-alpha (p-I $\kappa$ B $\alpha$ ) in liver tissues. Nuclear proteins were used to test NF $\kappa$ B levels. Groups are as follows. I: saline; II: saline + CCl<sub>4</sub>; III: AEOV 125mg/kg + CCl<sub>4</sub>; IV: AEOV 250 mg/kg + CCl<sub>4</sub>; V: AEOV 500 mg/kg + CCl<sub>4</sub>; VI: biphenyldicarboxylate 150 mg/kg + CCl<sub>4</sub>. (C) Immunohistochemical staining of NF $\kappa$ B in liver tissues. Groups are as follows. A: saline; B: saline + CCl<sub>4</sub>; C: AEOV 125 mg/kg + CCl<sub>4</sub>; D: AEOV 250 mg/kg + CCl<sub>4</sub>; E: AEOV 500 mg/kg + CCl<sub>4</sub>; F: biphenyldicarboxylate 150 mg/kg + CCl<sub>4</sub>.

### 2.5. Cytoprotective Effect of Epigallocatechin gallate against H<sub>2</sub>O<sub>2</sub>-Induced HepG2 Cells

In order to evaluate the probable cytotoxicity of epigallocatechin gallate on HepG2 cells, cell viability was measured after HepG2 cells were treated with different concentrations of epigallocatechin gallate for 12 h. As shown in Figure 6A, there was no inhibitory effect on the viability of HepG2 cells after exposure to epigallocatechin gallate at the concentrations of 193–774  $\mu$ M for 12 h.

Figure 6B indicates the cytoprotective effect of epigallocatechin gallate on HepG2 cells against the oxidative damage induced by H<sub>2</sub>O<sub>2</sub>. The exposure of HepG2 cells to 0.4 mM H<sub>2</sub>O<sub>2</sub> for 2 h significantly reduced the cell viability. Pretreatment of HepG2 cells with epigallocatechin gallate at the concentrations of 193–774  $\mu$ M remarkably decreased the cytotoxicity resulted from the exposure to H<sub>2</sub>O<sub>2</sub>. Notably, levels of lactate dehydrogenase (LDH) and malondialdehyde (MDA) elevated in H<sub>2</sub>O<sub>2</sub>-induced HepG2 cells, which

reflected marked increase of cell death. However, when HepG2 cells were pretreated with epigallocatechin gallate (EGCG), LDH and MDA levels reduced markedly, almost comparable to those of the control cells.

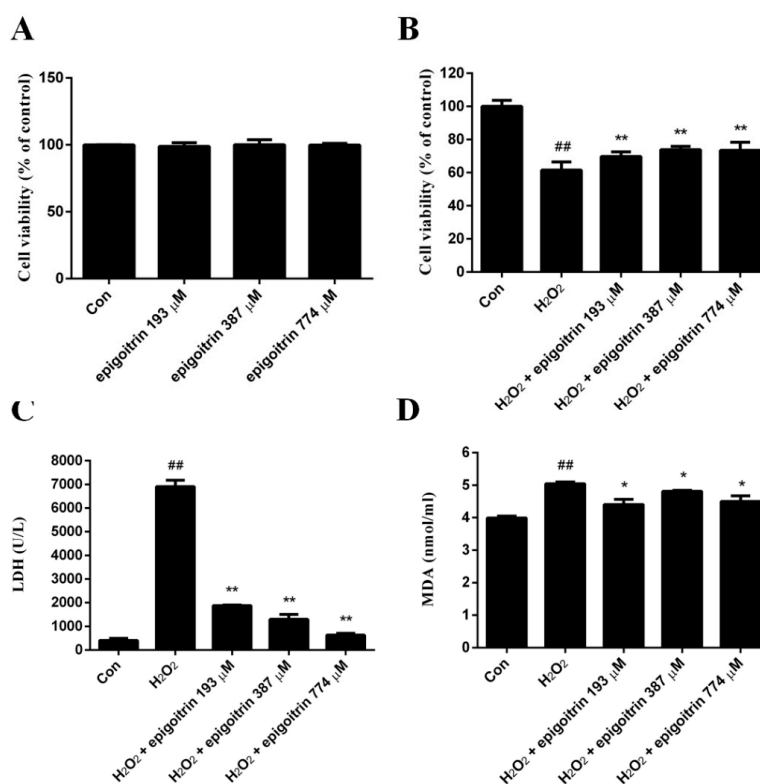


**Figure 6.** Cytoprotective effect of epigallocatechin gallate against H<sub>2</sub>O<sub>2</sub>-induced HepG2 cells. (A) Effect of epigallocatechin gallate on HepG2 cells viability determined by 3-(4,5-dimethylthiazol-2-yl)-2,5-diphenyltetrazolium bromide (MTT) assay. Cells were cultured with different concentrations of the epigallocatechin gallate (193, 387, and 774 μM) for 12 h. Values are the means ± SEM of three independent experiments; (B) Effect of epigallocatechin gallate on the viability of HepG2 cells with H<sub>2</sub>O<sub>2</sub> exposure. Cells were incubated with H<sub>2</sub>O<sub>2</sub> (0.4 mM, for 2 h) after pretreatment with epigallocatechin gallate (193, 387, and 774 μM) for 12 h. The cell viability was determined by the MTT assay. Values are the means ± SEM of three independent experiments. ## *p* < 0.01 versus control (untreated cells), \*\* *p* < 0.01 versus H<sub>2</sub>O<sub>2</sub>-treated cells. Effect of epigallocatechin gallate on lactate dehydrogenase (LDH) (C) and malondialdehyde (MDA) (D) levels in H<sub>2</sub>O<sub>2</sub>-induced HepG2 cells. Values are the means ± SEM of three independent experiments. ## *p* < 0.01 versus control (untreated cells), \*\* *p* < 0.01, \* *p* < 0.05 versus H<sub>2</sub>O<sub>2</sub> treated cells.

## 2.6. Anti-Oxidative and Anti-Inflammatory Effects of Epigallocatechin Gallate against H<sub>2</sub>O<sub>2</sub>-Induced HepG2 Cells

As shown in Figure 7A,B, H<sub>2</sub>O<sub>2</sub> administration significantly reduced superoxide dismutase (SOD) and GSH-Px activities in HepG2 cells compared with the control group. Epigallocatechin gallate pretreatment dose-dependently induced marked increase of SOD and GSH-Px activities. Similarly, when H<sub>2</sub>O<sub>2</sub>-induced HepG2 cells were pretreated with epigallocatechin gallate, the expression of Nrf2 and GCL appeared to continuously increase in comparison with the H<sub>2</sub>O<sub>2</sub>-treated cells (Figure 7C).

Expression of p-IκBα and NFκB was markedly elevated after HepG2 cells were treated with H<sub>2</sub>O<sub>2</sub>. With epigallocatechin gallate pretreatment, levels of p-IκBα and NFκB (Figure 7C), decreased significantly in a dose-dependent manner, indicating a significant anti-inflammatory effect of epigallocatechin gallate against H<sub>2</sub>O<sub>2</sub>-induced HepG2 cells.



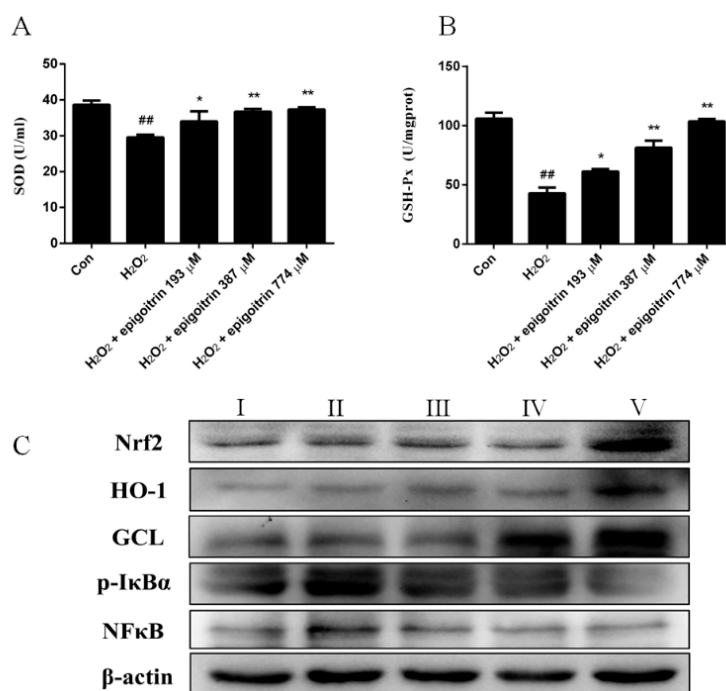


**Figure 7.** Anti-oxidative and anti-inflammatory effects of epigallocatechin against H<sub>2</sub>O<sub>2</sub>-induced HepG2 cells. (A,B) Effect of epigallocatechin on superoxide dismutase (SOD) and GSH-Px activities in H<sub>2</sub>O<sub>2</sub>-induced HepG2 cells. Values are the means  $\pm$  SEM of three independent experiments. <sup>##</sup>  $p < 0.01$  versus control (untreated cells), <sup>\*\*</sup>  $p < 0.01$ , <sup>\*</sup>  $p < 0.05$  versus H<sub>2</sub>O<sub>2</sub>-treated cells; (C) Effect of epigallocatechin on the expression of Nrf2, GCL, HO-1, p-I $\kappa$ B $\alpha$ , and NF $\kappa$ B in H<sub>2</sub>O<sub>2</sub>-induced HepG2 cells. Cells were treated with H<sub>2</sub>O<sub>2</sub> (0.4 mM, for 2 h) after pretreatment with epigallocatechin for 12 h. Protein expression was then detected by western blot analysis. Groups are as follows. I: saline; II: saline + H<sub>2</sub>O<sub>2</sub>; III: epigallocatechin 193  $\mu$ M + H<sub>2</sub>O<sub>2</sub>; IV: epigallocatechin 387  $\mu$ M + H<sub>2</sub>O<sub>2</sub>; V: epigallocatechin 774  $\mu$ M + H<sub>2</sub>O<sub>2</sub>.

### 3. Discussion

To the best of our knowledge, no study has been reported on the hepatoprotective effect of AEOV. Thus, the present study was performed to investigate the hepatoprotective effect of AEOV *in vivo* using CCl<sub>4</sub>-induced mouse model and evaluate the cytoprotective effect *in vitro* using H<sub>2</sub>O<sub>2</sub>-induced HepG2 cells, and further explore the underlying mechanism. AEOV helped to attenuate liver injury induced by CCl<sub>4</sub> in a dose-dependent manner. Epigallocatechin exhibited strong cytoprotective effect against H<sub>2</sub>O<sub>2</sub>-induced oxidative damage in HepG2 cells. Additional study revealed that hepatoprotective actions of AEOV and epigallocatechin were largely related to their strong anti-oxidative and anti-inflammatory properties via regulation of Nrf2 and NF $\kappa$ B pathways (Figure 8).

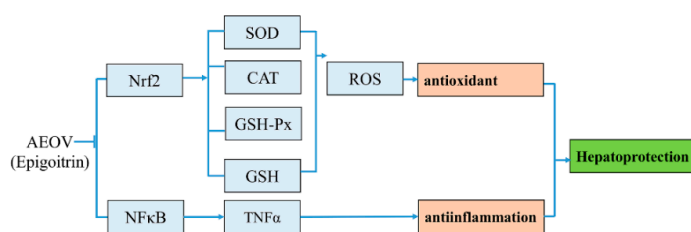


**Figure 8.** A schematic illustration of a proposed mechanism.

Alkaloids and organic acids are two major chemical portions of AEOV. Naturally occurring alkaloids widely isolated from numerous common medicinal plants, have long been known to exert a broad spectrum of pharmacological properties, including anti-endotoxic, antiviral, anticancer,

antinociceptive, anti-inflammatory, antimalarial, and antipyretic effects [19,20]. Protocatechuic acid and caffeic acid are the major organic acid constituents isolated from AEOV. They are also derived from various Chinese herbal medicines, and are reported to activate anti-oxidative genes that combat oxidative stress and cell apoptosis [21,22]. Alkaloids may chemically react with organic acids *in vivo*, producing a better pharmacological effect. Consequently, AEOV, a mixture of alkaloids and organic acids, holds promise as a hepatoprotective agent. In the present study, we found that AEOV pretreatment restored liver injury induced by CCl<sub>4</sub> in a dose-dependent manner, and levels of ALT and AST in serum were also substantially decreased with AEOV pretreatment, firmly confirming the hepatoprotective effect of AEOV *in vivo*. Moreover, the cytoprotective effect *in vitro* was demonstrated in H<sub>2</sub>O<sub>2</sub>-induced HepG2 cells using epigallocatechin gallate, the major polyphenolic compound isolated from AEOV. Previous screenings showed that epigallocatechin gallate had strong inhibitory effect on influenza virus [23]. However, here, we demonstrated the cytoprotective, anti-oxidative, and anti-inflammatory effects of epigallocatechin gallate against H<sub>2</sub>O<sub>2</sub>-induced oxidative damage in HepG2 cells.

Accumulating evidence suggests that ROS-induced oxidative stress plays a central role in several human pathologies including liver injury, causing the peroxidation of lipids, protein oxidation, DNA damage, mitochondrial dysfunction and altered signal transduction [24–26]. Hence, effective therapeutic approaches are urgently needed to inhibit the detrimental effect of ROS, for instance, through the induction of endogenous enzymatic antioxidants [27]. Nrf2, a basic region-leucine zipper (CNC bZip) transcription factor, plays a key role in modulating cellular defense against oxidative stress [28–30]. Under normal conditions, Nrf2 is retained in the cytoplasm by binding to its negative regulator, Keap1. The production of ROS typically provokes a cellular oxidative stress environment, which causes dissociation of Keap1 from Nrf2, thereby allowing Nrf2 to translocate into the nucleus [31,32], activating antioxidant genes and enzymes including glutathione peroxidase (GPx), glutathione-S-transferase (GST), heme oxygenase (HO), glutamate cysteine ligase (GCLc) and superoxide dismutase (SOD) by binding to antioxidant response elements (ARE) in the promoter regions of its target genes [33–35], which subsequently contributes to adaptation and protection of cells against oxidative stress [36]. In the present study, we found that AEOV enhanced nuclear translocation of Nrf2, decreased level of Keap1, and elevated expression of HO-1 and GCL, indicating involvement of the Nrf2-ARE pathway in AEOV-mediated hepatoprotective effect *in vivo*. Moreover, T-SOD, CAT, GSH-Px, and GSH, playing essential roles in detoxifying the reactive toxic metabolites of many toxins, were substantially elevated by AEOV treatment, confirming the anti-oxidative property of AEOV in liver tissues of CCl<sub>4</sub>-induced mice. In addition, activities of SOD and GSH-Px and expression of Nrf2 and GCL were also elevated significantly with epigallocatechin gallate pretreatment in H<sub>2</sub>O<sub>2</sub>-induced HepG2 cells, which indicated the anti-oxidative effect of epigallocatechin gallate *in vitro*.

It has been well established that an excessive inflammatory reaction, including the release of pro-inflammatory cytokine such as TNF- $\alpha$ , is largely responsible for liver injury [37–39]. The inflammatory response is mainly triggered by NF $\kappa$ B, a pleiotropic regulator of various genes encoding inflammatory mediators [40–42]. In an unstimulated state, NF $\kappa$ B is stabilized in cytosol by inhibitory factor  $\kappa$ B- $\alpha$  (I $\kappa$ B $\alpha$ ) [42]. After being activated by various inducers including cytokines, reactive oxygen species (ROS) and bacterial lipopolysaccharides, I $\kappa$ B $\alpha$  becomes phosphorylated triggering its proteolytic degradation, leading to transient translocation of NF $\kappa$ B from the cytoplasm to the nucleus, thus activating the expression of pro-inflammatory proteins, cytokines, chemokines, adhesion molecules or enzymes involved in the inflammatory process [43–47]. In the present study we found that treatment with AEOV *in vivo* reduced the overall nuclear localization of NF $\kappa$ B via reducing IKK $\alpha$  and inhibiting the phosphorylation and degradation of I $\kappa$ B $\alpha$ , thereby precluding the expression of NF $\kappa$ B target genes, rescuing cells from inflammatory injuries. Additionally, expression of p-I $\kappa$ B $\alpha$  and NF $\kappa$ B also decreased significantly with epigallocatechin gallate pretreatment in H<sub>2</sub>O<sub>2</sub>-induced HepG2 cells. Taken together, with our results, the hepatoprotective effect of AEOV *in vivo* and the cytoprotective effect of epigallocatechin gallate in HepG2 cells are specifically related to the observed anti-inflammatory effect as supported by the strong inhibition of NF $\kappa$ B pathway.

In summary, we successfully demonstrated the potent protective effect of AEOV against  $\text{CCl}_4$ -induced liver injury and confirmed the cytoprotective effect of epigoitrin in HepG2 cells. The hepatoprotective effect of AEOV in vivo and the cytoprotective effect of epigoitrin in  $\text{H}_2\text{O}_2$ -induced HepG2 cells were associated with their strong anti-oxidative and anti-inflammatory properties via enhancing the Nrf2 response and inhibiting the  $\text{NF}\kappa\text{B}$  signaling pathway. Epigoitrin, as a major component of AEOV may be partially responsible for the anti-oxidative and anti-inflammatory effects of AEOV, which needs further investigation.

## 4. Methods

### 4.1. Plant Material and Extract Preparation

Seeds of *O. violaceus* were collected in Beijing province, People's Republic of China, in August 2015. The material was identified and authenticated by Wan-Long Ding. A voucher specimen (NO. 150811) was deposited at the Institute of Medicinal Plant Development, Chinese Academy of Medical Science and Peking Union Medical College (Beijing, China). To prepare aqueous extract, the air-dried and powdered seeds of *O. violaceus* (20.0 kg) were extracted three times with water ( $3 \times 40$  L, 2 h each), then the solvent was evaporated using a rotary evaporator. The obtained extract was freeze-dried and stored at  $-20$  °C.

### 4.2. HPLC Analysis

After extraction with water, the aqueous extract was concentrated to the small volume (3 L), and applied on a D-101 macroporous adsorptive resin (20 kg,  $20 \times 200$  cm), eluting with  $\text{H}_2\text{O}$  (60 L) and 10% EtOH (80 L). The 10% EtOH fraction was concentrated under reduced pressure, and the residue (400 g) was subjected to column chromatography (CC) on silica gel (100–200 mesh,  $15 \times 60$  cm) eluting with a stepwise gradient of  $\text{CH}_2\text{Cl}_2/\text{CH}_3\text{OH}$  (10:1 to 1:1, 5 L) to obtain eight fractions (Fr. A–Fr. H). Fr. F (30 g) was subjected to chromatography using ODS MPLC (ODS Medium Pressure Preparative Liquid Chromatography) elution with  $\text{MeOH-H}_2\text{O}$  (10:90; 30:70; 50:50), yielding three fractions (Fr. F1–3). Fr. F1 (5.7 g) was separated by a Sephadex LH-20 column ( $5 \times 80$  cm), eluted with  $\text{MeOH}$ , and then purified by preparative HPLC affording compounds 1 (15.6 mg), 2 (10.2 mg), and 3 (11.8 mg). Fr. F2 (4.6 g) was separated via reverse-phase chromatography over C-18 silica gel, eluted with  $\text{MeOH-H}_2\text{O}$  (10:90; 30:70), and then purified through preparative HPLC elution using a  $\text{MeOH-H}_2\text{O}$  (25:75) system and a Kromasil RP-18 column. Finally, compounds 4, 5 (15.3 mg), 6, 7 (10.8 mg), 8 (11.1 mg), 9 (5.4 mg), 10 (10.1 mg), 11 (9.4 mg), 12 (8.9 mg), 13 (5.7 mg), and 14 (10.1 mg) were obtained. Their structures were elucidated by spectroscopic analysis and comparison with data in the literature.

### 4.3. Cell Culture

Human HepG2 cells were cultured in Dulbecco's Modified Eagle Medium (DMEM) supplemented with 10% fetal bovine serum (FBS), 100 U/mL penicillin and 100  $\mu\text{g}/\text{mL}$  streptomycin at 37 °C in an atmosphere of 5%  $\text{CO}_2$ .

### 4.4. Cell Viability Evaluation

Initially, the probable cytotoxicity of epigoitrin (193 to 774  $\mu\text{M}$ ) on HepG2 cells was assessed using the 3-(4,5-dimethylthiazol-2-yl)-2,5-diphenyltetrazolium bromide (MTT) method. Briefly, 24 h after being seeded in 96-well plates, cells were treated with epigoitrin at different concentrations (193, 387, and 774  $\mu\text{M}$ ) for 12 h. Then, the medium was removed, and the cells were washed with phosphate buffered saline (PBS), followed by MTT (0.5 mg/mL) incubation for an additional 4 h. Then the MTT-formazan product was dissolved in 150  $\mu\text{L}$  of dimethyl sulfoxide and the optical density of the solution was measured at 570 nm using a microplate spectrophotometer.

Next, the cytoprotective effect of epigoitrin on H<sub>2</sub>O<sub>2</sub>-induced HepG2 cells was evaluated. Following the exposure to epigoitrin (193 to 774 µM) for 12 h, cells were washed and treated with H<sub>2</sub>O<sub>2</sub> (0.4 mM) for another 2 h. Cell viability was then assessed by MTT method. The cells without treatment with epigoitrin or H<sub>2</sub>O<sub>2</sub> were considered as control with cell viability of 100 %. Cell viability was determined as a percentage of viable cells of treated wells to control wells.

#### 4.5. Measurement of LDH, MDA, SOD, and GSH-Px in H<sub>2</sub>O<sub>2</sub>-Induced HepG2 Cells

HepG2 cells were pretreated by different concentrations of epigoitrin (193, 387, and 774 µM) for 12 h and then exposed to 0.4 mM H<sub>2</sub>O<sub>2</sub> for 2 h. The supernatant was then used for LDH detection. After preparing cell lysates by repeated freeze-thaw cycles, the MDA, SOD, GSH-Px activities were evaluated in a 96-well plate using their respective activity assay kits (Nanjing Jiancheng Bioengineering Institute, Nanjing, China) following the manufacturer's instructions.

#### 4.6. Animals

Male Balb/c mice were obtained from Vital River Laboratory Animal Technology Co., Ltd. (Beijing, China). Animals were kept in a 12 h light/dark cycle under standard conditions with free access to food and water. All animal care and experimental protocols used in this study were approved by the Institutional Animal Care and Use Committee at the Institute of Medicinal Plant Development, Chinese Academy of Medical Sciences (SLXD-2015111972, 19 November 2015).

#### 4.7. Induction of CCl<sub>4</sub>-Mediated Liver Injury

Mice were randomly divided into six different groups ( $n = 8$ ) and orally administrated with relevant drugs for 4 days: Group I (normal control group, saline), Group II (model group, saline), Group III (AEOV 125 mg/kg), Group IV (AEOV 250 mg/kg), Group V (AEOV 500 mg/kg), and Group VI (biphenyldicarboxylate 150 mg/kg, Beijing Union Pharmaceutical Factory, Beijing, China). Subsequently, mice in Groups II-VI were given a single intraperitoneal injection of 0.1% CCl<sub>4</sub> (10 µL/g, dissolved in olive oil). Meanwhile, mice in Group I were intraperitoneally injected with vehicle (10 µL/g, olive oil).

#### 4.8. Liver Weight and Liver Index

Sixteen hours after CCl<sub>4</sub> injection, mice were weighed and sacrificed. Livers were then collected and weighed to calculate liver index using the following formula: Liver index = liver weight/body weight × 100%

Small portions of each liver were routinely processed for histological examinations, and other portions were kept at −20 °C.

#### 4.9. Serum Biochemistry

Serum ALT and AST were assayed using commercially available test kits with a biochemistry analyzer system according to the manufacturer's instructions.

#### 4.10. Assay of Reactive Oxygen Species (ROS) and Hepatic Enzymes in Liver Tissues

Livers were homogenized in nine volumes of ice-cold normal saline. The homogenate was centrifuged at 4 °C (4000 r/min, 10 min), and the resultant supernatant was used for the assay of hepatic enzymes. The activities of SOD, CAT, GSH-Px, and GSH and the level of ROS were determined using their respective activity assay kits (Nanjing Jiancheng Bioengineering Institute, Nanjing, China) following the manufacturer's instructions.

#### 4.11. Histological Analysis

Liver tissues were fixed in 10% formaldehyde solution. The fixed tissues were then embedded in paraffin and cut into 3  $\mu$ m sections which were then deparaffinized in xylene and rehydrated in a graded series of ethanol. The severity of liver injury was assessed by morphometric evaluation of liver slides with hematoxylin and eosin staining.

#### 4.12. Immunohistochemical Analyses

For immunohistochemistry, the sections were blocked with a buffered blocking solution (3% bovine serum albumin in phosphate-buffered saline (PBS) for 15 min. After blocking, sections were incubated with the primary antibodies for NF $\kappa$ B (1:50) and Nrf2 (1:50) at 4 °C overnight, followed by washing with PBS and co-incubation with a secondary antibody at room temperature for 1 h. Then, sections were visualized with 3',3'-diaminobenzidine and nuclei were then counterstained with hematoxylin. The Image-ProPlus 4.5 Software (Media Cybernetics) was used to analyze the expression of proteins.

#### 4.13. Western Blot Analysis

Liver tissues and HepG2 cells were homogenized in a standard RIPA buffer supplemented with a cocktail of protease and phosphatase inhibitors. The protein concentrations of the extracts were determined using a BCA (Bicin-chonic Acid) Protein Assay reagent kit (Beyotime Biotech, Nanjing, China). An equal amount of total protein per lane was fractionated on an 8% sodium dodecyl sulfate-polyacrylamide gel. After electrophoresis, the gels were transferred onto polyvinylidene difluoride membranes, which were then blocked with Tris-buffered saline containing 5% nonfat milk at 4 °C for 2 h. The membranes were incubated with primary antibodies (1:300) over night at 4 °C. After washing three times, the membranes were incubated with horseradish peroxidase (HRP)-conjugated secondary antibodies at room temperature for 1 h and subsequently processed for enhanced chemiluminescence (ECL) detection using a commercial kit (Beyotime Biotech, Nanjing, China). Signals were detected using a chemiluminescence system (Bio-Rad, Hercules, CA, USA).  $\beta$ -actin content was used as an internal control.

#### 4.14. Statistical Analysis

The data were presented as means  $\pm$  standard error and compared by one way analysis of variance. Significant difference between groups was determined using Duncan's test. Differences were considered to be statistically significant when  $p < 0.05$ .

**Acknowledgments:** This work was financially supported by Beijing Natural Science Foundation (No.7164281), the Technological Large Platform for Comprehensive Research and Development of New Drugs in the Twelfth Five-Year "Significant New Drugs Created" Science and Technology Major Projects (No. 2012ZX09301-002-001-033), and the Technological Large Platform for Comprehensive Research and Development of New Drugs in the CAMS Innovation Fund for Medical Science (CIFMS) (Grant No. 2016-I2M-1-012). This work was also supported by Key Laboratory of Bioactive Substances and Resources Utilization of Chinese Herbal Medicine, Ministry of Education, and by Beijing Key Laboratory of Innovative Drug Discovery of Traditional Chinese Medicine (Natural Medicine) and Translational Medicine, Institute of Medical Plant Development, Peking Union Medical College and Chinese Academy of Medical Sciences.

**Author Contributions:** Nailiang Zhu and Li Cao conceived and designed the experiments. Chenqi Liu and Xiaowei Huo performed the experiments. Li Gao and Xudong Xu analyzed the data. Xiaowei Huo wrote the manuscript. All authors reviewed the manuscript.

**Conflicts of Interest:** The authors declare no conflict of interest.

## References

1. Zhou, Y.X.; Qiu, Y.Q.; Xu, L.Q.; Guo, J.; Li, L.J. Xiao-chai-hu tang in treating model mice with D-galactosamine-induced liver injury. *Afr. J. Tradit. Complement. Altern. Med.* **2012**, *9*, 405–411. [[CrossRef](#)] [[PubMed](#)]

2. Kusunose, M.; Qiu, B.; Cui, T.; Hamada, A.; Yoshioka, S.; Ono, M.; Miyamura, M.; Kyotani, S.; Nishioka, Y. Effect of sho-saiko-to extract on hepatic inflammation and fibrosis in dimethylnitrosamine induced liver injury rats. *Biol. Pharm. Bull.* **2002**, *25*, 1417–1421. [[CrossRef](#)] [[PubMed](#)]
3. Arteel, G.E. Oxidants and antioxidants in alcohol-induced liver disease. *Gastroenterology* **2003**, *124*, 778–790. [[CrossRef](#)] [[PubMed](#)]
4. Dey, A.; Cederbaum, A.I. Alcohol and oxidative liver injury. *Hepatology* **2006**, *43*, S63–S74. [[CrossRef](#)] [[PubMed](#)]
5. Miller, A.M.; Wang, H.; Park, O.; Horiguchi, N.; Lafdil, F.; Mukhopadhyay, P.; Moh, A.; Fu, X.Y.; Kunos, G.; Pacher, P.; et al. Anti-inflammatory and anti-apoptotic roles of endothelial cell STAT3 in alcoholic liver injury. *Alcohol. Clin. Exp. Res.* **2010**, *34*, 719–725. [[CrossRef](#)] [[PubMed](#)]
6. He, Y.M.; Zhu, S.; Ge, Y.W.; Kazuma, K.; Zou, K.; Cai, S.Q.; Komatsu, K. The anti-inflammatory secoiridoid glycosides from *Gentiana Scabrae Radix*: The root and rhizome of *Gentiana scabra*. *J. Nat. Med.* **2015**, *69*, 303–312. [[CrossRef](#)] [[PubMed](#)]
7. Jeong, Y.T.; Jeong, S.C.; Hwang, J.S.; Kim, J.H. Modulation effects of sweroside isolated from the *Lonicera japonica* on melanin synthesis. *Chem. Biol. Interact.* **2015**, *238*, 33–39. [[CrossRef](#)] [[PubMed](#)]
8. Parsons, C.J.; Takashima, M.; Rippe, R.A. Molecular mechanisms of hepatic fibrogenesis. *J. Gastroenterol. Hepatol.* **2007**, *22* (Suppl. S1), S79–S84. [[CrossRef](#)] [[PubMed](#)]
9. Jiang, Y.M.; Wang, Y.; Tan, H.S.; Yu, T.; Fan, X.M.; Chen, P.; Zeng, H.; Huang, M.; Bi, H.C. Schisandrol B protects against acetaminophen-induced acute hepatotoxicity in mice via activation of the Nrf2/ARE signaling pathway. *Acta Pharmacol. Sin.* **2016**, *37*, 382–389. [[CrossRef](#)] [[PubMed](#)]
10. Chen, X.L.; Dodd, G.; Thomas, S.; Zhang, X.; Wasserman, M.A.; Rovin, B.H.; Kunsch, C. Activation of Nrf2/ARE pathway protects endothelial cells from oxidant injury and inhibits inflammatory gene expression. *Am. J. Physiol. Heart Circ. Physiol.* **2006**, *290*, H1862–H1870. [[CrossRef](#)] [[PubMed](#)]
11. Enomoto, A.; Itoh, K.; Nagayoshi, E.; Haruta, J.; Kimura, T.; O'Connor, T.; Harada, T.; Yamamoto, M. High sensitivity of Nrf2 knockout mice to acetaminophen hepatotoxicity associated with decreased expression of are-regulated drug metabolizing enzymes and antioxidant genes. *Toxicol. Sci.* **2001**, *59*, 169–177. [[CrossRef](#)] [[PubMed](#)]
12. Rahman, I.; Biswas, S.K.; Kirkham, P.A. Regulation of inflammation and redox signaling by dietary polyphenols. *Biochem. Pharmacol.* **2006**, *72*, 1439–1452. [[CrossRef](#)] [[PubMed](#)]
13. Kodali, P.; Wu, P.; Lahiji, P.A.; Brown, E.J.; Maher, J.J. Anit toxicity toward mouse hepatocytes in vivo is mediated primarily by neutrophils via CD18. *Am. J. Physiol. Gastrointest. Liver Physiol.* **2006**, *291*, G355–G363. [[CrossRef](#)] [[PubMed](#)]
14. Yang, Q.L.; Yang, F.; Gong, J.T.; Tang, X.W.; Wang, G.Y.; Wang, Z.T.; Yang, L. Sweroside ameliorates  $\alpha$ -naphthylisothiocyanate-induced cholestatic liver injury in mice by regulating bile acids and suppressing pro-inflammatory responses. *Acta Pharmacol. Sin.* **2016**, *37*, 1218–1228. [[CrossRef](#)] [[PubMed](#)]
15. Hirschfield, G.M.; Heathcote, E.J.; Gershwin, M.E. Pathogenesis of cholestatic liver disease and therapeutic approaches. *Gastroenterology* **2010**, *139*, 1481–1496. [[CrossRef](#)] [[PubMed](#)]
16. Rahim, S.M.; Taha, E.M.; Al-janabi, M.S.; Al-douri, B.I.; Simon, K.D.; Mazlan, A.G. Hepatoprotective effect of cymbopogon citratus aqueous extract against hydrogen peroxide-induced liver injury in male rats. *Afr. J. Tradit. Complement. Altern. Med.* **2014**, *11*, 447–451. [[CrossRef](#)] [[PubMed](#)]
17. Hua, Y.W.; Liu, M.; Li, Z.Y. Parental genome separation and elimination of cells and chromosomes revealed by AFLP and GISH analyses in a *Brassica carinata*  $\times$  *Orychophragmus violaceus* cross. *Ann. Bot.* **2006**, *97*, 993–998. [[CrossRef](#)] [[PubMed](#)]
18. Zhan, Y.W.; Xu, Z.Q.; Guo, X.H.; Li, R.J.; Shen, J.G.; Xu, X.D.; Zhang, B.X. Protective effect of aqueous extract from the seeds of *Orychophragmus violaceus* against acute liver injury induced by *Cortex dictamni* in mice. *Chin. J. Pharmacol. Toxicol.* **2016**, *30*, 101–106.
19. Pingali, S.; Donahue, J.P.; Payton-Stewart, F. Tetrahydroberberine, a pharmacologically active naturally occurring alkaloid. *Acta Crystallogr. C Struct. Chem.* **2015**, *71*, 262–265. [[CrossRef](#)] [[PubMed](#)]
20. Xiao, P.; Huang, H.; Chen, J.; Li, X. In vitro antioxidant and anti-inflammatory activities of *Radix isatidis* extract and bioaccessibility of six bioactive compounds after simulated gastro-intestinal digestion. *J. Ethnopharmacol.* **2014**, *157*, 55–61. [[CrossRef](#)] [[PubMed](#)]

21. Masella, R.; Santangelo, C.; D'Archivio, M.; Li Volti, G.; Giovannini, C.; Galvano, F. Protocatechuic acid and human disease prevention: Biological activities and molecular mechanisms. *Curr. Med. Chem.* **2012**, *19*, 2901–2917. [[CrossRef](#)] [[PubMed](#)]
22. Giovannini, C.; Scazzocchio, B.; Matarrese, P.; Vari, R.; D'Archivio, M.; Di Benedetto, R.; Casciani, S.; Dessi, M.R.; Straface, E.; Malorni, W.; et al. Apoptosis induced by oxidized lipids is associated with up-regulation of p66Shc in intestinal Caco-2 cells: Protective effects of phenolic compounds. *J. Nutr. Biochem.* **2008**, *19*, 118–128. [[CrossRef](#)] [[PubMed](#)]
23. Xiao, P.; Ye, W.; Chen, J.; Li, X. Antiviral activities against influenza virus (FM1) of bioactive fractions and representative compounds extracted from Banlangen (*Radix isatidis*). *J. Tradit. Chin. Med.* **2016**, *36*, 369–376. [[PubMed](#)]
24. Park, C.H.; Tanaka, T.; Cho, E.J.; Park, J.C.; Shibahara, N.; Yokozawa, T. Glycerol-induced renal damage improved by 7-O-galloyl-D-sedoheptulose treatment through attenuating oxidative stress. *Biol. Pharm. Bull.* **2012**, *35*, 34–41. [[CrossRef](#)] [[PubMed](#)]
25. Sporn, M.B.; Liby, K.T. Cancer chemoprevention: Scientific promise, clinical uncertainty. *Nat. Clin. Pract. Oncol.* **2005**, *2*, 518–525. [[CrossRef](#)] [[PubMed](#)]
26. Liu, M.; Ravula, R.; Wang, Z.; Zuo, Z.; Chow, M.S.; Thakkar, A.; Prabhu, S.; Andresen, B.; Huang, Y. Traditional chinese medicinal formula si-wu-tang prevents oxidative damage by activating Nrf2-mediated detoxifying/antioxidant genes. *Cell. Biosci.* **2014**, *4*, 8. [[CrossRef](#)] [[PubMed](#)]
27. Nair, S.; Doh, S.T.; Chan, J.Y.; Kong, A.N.; Cai, L. Regulatory potential for concerted modulation of Nrf2- and NFκB1-mediated gene expression in inflammation and carcinogenesis. *Br. J. Cancer* **2008**, *99*, 2070–2082. [[CrossRef](#)] [[PubMed](#)]
28. Kobayashi, M.; Yamamoto, M. Molecular mechanisms activating the Nrf2-keap1 pathway of antioxidant gene regulation. *Antioxid. Redox Signal.* **2005**, *7*, 385–394. [[CrossRef](#)] [[PubMed](#)]
29. Sekhar, K.R.; Yan, X.X.; Freeman, M.L. Nrf2 degradation by the ubiquitin proteasome pathway is inhibited by KIAA0132, the human homolog to INrf2. *Oncogene* **2002**, *21*, 6829–6834. [[CrossRef](#)] [[PubMed](#)]
30. Hong, Y.; Yan, W.; Chen, S.; Sun, C.R.; Zhang, J.M. The role of Nrf2 signaling in the regulation of antioxidants and detoxifying enzymes after traumatic brain injury in rats and mice. *Acta Pharmacol. Sin.* **2010**, *31*, 1421–1430. [[CrossRef](#)] [[PubMed](#)]
31. Niture, S.K.; Kaspar, J.W.; Shen, J.; Jaiswal, A.K. Nrf2 signaling and cell survival. *Toxicol. Appl. Pharmacol.* **2010**, *244*, 37–42. [[CrossRef](#)] [[PubMed](#)]
32. Kobayashi, M.; Yamamoto, M. Nrf2-keap1 regulation of cellular defense mechanisms against electrophiles and reactive oxygen species. *Adv. Enzyme Regul.* **2006**, *46*, 113–140. [[CrossRef](#)] [[PubMed](#)]
33. Patterson, A.D.; Carlson, B.A.; Li, F.; Bonzo, J.A.; Yoo, M.H.; Krausz, K.W.; Conrad, M.; Chen, C.; Gonzalez, F.J.; Hatfield, D.L. Disruption of thioredoxin reductase 1 protects mice from acute acetaminophen-induced hepatotoxicity through enhanced Nrf2 activity. *Chem. Res. Toxicol.* **2013**, *26*, 1088–1096. [[CrossRef](#)] [[PubMed](#)]
34. Goldring, C.E.; Kitteringham, N.R.; Elsby, R.; Randle, L.E.; Clement, Y.N.; Williams, D.P.; McMahon, M.; Hayes, J.D.; Itoh, K.; Yamamoto, M.; et al. Activation of hepatic Nrf2 in vivo by acetaminophen in CD-1 mice. *Hepatology* **2004**, *39*, 1267–1276. [[CrossRef](#)] [[PubMed](#)]
35. Kansanen, E.; Kivela, A.M.; Levonen, A.L. Regulation of Nrf2-dependent gene expression by 15-deoxy- $\delta$ 12,14-prostaglandin J2. *Free Radic. Biol. Med.* **2009**, *47*, 1310–1317. [[CrossRef](#)] [[PubMed](#)]
36. Chan, K.; Han, X.D.; Kan, Y.W. An important function of Nrf2 in combating oxidative stress: Detoxification of acetaminophen. *Proc. Natl. Acad. Sci. USA* **2001**, *98*, 4611–4616. [[CrossRef](#)] [[PubMed](#)]
37. Hill, D.A.; Jean, P.A.; Roth, R.A. Bile duct epithelial cells exposed to  $\alpha$ -naphthylisothiocyanate produce a factor that causes neutrophil-dependent hepatocellular injury in vitro. *Toxicol. Sci.* **1999**, *47*, 118–125. [[CrossRef](#)] [[PubMed](#)]
38. Wang, T.; Zhou, Z.X.; Sun, L.X.; Li, X.; Xu, Z.M.; Chen, M.; Zhao, G.L.; Jiang, Z.Z.; Zhang, L.Y. Resveratrol effectively attenuates  $\alpha$ -naphthyl-isothiocyanate-induced acute cholestasis and liver injury through choleric and anti-inflammatory mechanisms. *Acta Pharmacol. Sin.* **2014**, *35*, 1527–1536. [[CrossRef](#)] [[PubMed](#)]
39. Dahm, L.J.; Schultze, A.E.; Roth, R.A. An antibody to neutrophils attenuates  $\alpha$ -naphthylisothiocyanate-induced liver injury. *J. Pharmacol. Exp. Ther.* **1991**, *256*, 412–420. [[PubMed](#)]

40. Rogler, G.; Brand, K.; Vogl, D.; Page, S.; Hofmeister, R.; Andus, T.; Knuechel, R.; Baeuerle, P.A.; Scholmerich, J.; Gross, V. Nuclear factor  $\kappa$ B is activated in macrophages and epithelial cells of inflamed intestinal mucosa. *Gastroenterology* **1998**, *115*, 357–369. [[CrossRef](#)]
41. Barnes, P.J.; Karin, M. Nuclear factor- $\kappa$ B: A pivotal transcription factor in chronic inflammatory diseases. *N. Engl. J. Med.* **1997**, *336*, 1066–1071. [[CrossRef](#)]
42. Huo, X.; Zhang, L.; Gao, L.; Guo, Y.; Zhang, L.; Li, L.; Si, J.; Cao, L. Antiinflammatory and analgesic activities of ethanol extract and isolated compounds from *Milletia pulchra*. *Biol. Pharm. Bull.* **2015**, *38*, 1328–1336. [[CrossRef](#)] [[PubMed](#)]
43. Wardyn, J.D.; Ponsford, A.H.; Sanderson, C.M. Dissecting molecular cross-talk between Nrf2 and NF- $\kappa$ B response pathways. *Biochem. Soc. Trans.* **2015**, *43*, 621–626. [[CrossRef](#)]
44. Bolati, D.; Shimizu, H.; Yisireyili, M.; Nishijima, F.; Niwa, T. Indoxyl sulfate, a uremic toxin, downregulates renal expression of Nrf2 through activation of NF- $\kappa$ B. *BMC Nephrol.* **2013**, *14*, 56. [[CrossRef](#)] [[PubMed](#)]
45. Shimizu, H.; Bolati, D.; Higashiyama, Y.; Nishijima, F.; Shimizu, K.; Niwa, T. Indoxyl sulfate upregulates renal expression of MCP-1 via production of ROS and activation of NF- $\kappa$ B, p53, ERK, and JNK in proximal tubular cells. *Life Sci.* **2012**, *90*, 525–530. [[CrossRef](#)] [[PubMed](#)]
46. Winston, J.T.; Strack, P.; Beer-Romero, P.; Chu, C.Y.; Elledge, S.J.; Harper, J.W. The SCF $\beta$ -TRCP-ubiquitin ligase complex associates specifically with phosphorylated destruction motifs in I $\kappa$ B $\alpha$  and  $\beta$ -catenin and stimulates I $\kappa$ B $\alpha$  ubiquitination in vitro. *Genes Dev.* **1999**, *13*, 270–283. [[CrossRef](#)] [[PubMed](#)]
47. Hirai, S.; Horii, S.; Matsuzaki, Y.; Ono, S.; Shimmura, Y.; Sato, K.; Egashira, Y. Anti-inflammatory effect of pyroglutamyl-leucine on lipopolysaccharide-stimulated RAW 264.7 macrophages. *Life Sci.* **2014**, *117*, 1–6. [[CrossRef](#)] [[PubMed](#)]



© 2017 by the authors. Licensee MDPI, Basel, Switzerland. This article is an open access article distributed under the terms and conditions of the Creative Commons Attribution (CC BY) license (<http://creativecommons.org/licenses/by/4.0/>).